OPEN

Citation: Cell Death and Disease (2013) 4, e703; doi:10.1038/cddis.2013.218

www.nature.com/cddis

The purinergic $P2Y_{14}$ receptor axis is a molecular determinant for organism survival under *in utero* radiation toxicity

SH Kook[1,8,9], JS Cho[1,8], A Morrison[2], E Wiener[3], SB Lee[4], D Scadden[5,6,7] and B-C Lee*[,1]

In utero **exposure of the embryo and fetus to radiation has been implicated in malformations or fetal death, and often produces lifelong health consequences such as cancers and mental retardation. Here we demonstrate that deletion of a G-protein-coupled purinergic receptor, $P2Y_{14}$, confers potent resistance to *in utero* radiation. Intriguingly, a putative $P2Y_{14}$ receptor ligand, UDP-glucose, phenocopies the effect of $P2Y_{14}$ deficiency. These data indicate that $P2Y_{14}$ is a receptor governing *in utero* tolerance to genotoxic stress that may be pharmacologically targeted to mitigate radiation toxicity in pregnancy.**
Cell Death and Disease (2013) **4,** e703; doi:10.1038/cddis.2013.218; published online 4 July 2013
Subject Category: Experimental Medicine

The embryo is very susceptible to genotoxic stress, and even low levels of radiation can increase the risk of fetal damage. The incidence of miscarriage, preterm delivery and death during infancy are more common in pregnant women exposed to radiation. However, there are medical situations where pregnant women are intentionally exposed to radiation due to life-threatening conditions. The number of pregnant women undergoing computed tomography (CT) imaging, which delivers more radiation than other radiologic procedures, has nearly doubled in the past decade.[1] To date, shielding has been the only method for protecting the fetus against radiation injury. Nuclear accidents or terrorism can also place the fetus at significant risk.

Purinergic receptors are a family of transmembrane proteins that is activated by nucleosides, nucleotides, and nucleotide sugars. Purinergic receptors are divided into P1 adenosine receptor, P2X ionotropic receptor and P2Y metabotropic receptor.[2,3] Purines and pyrimidines are massively released at the site of damage resulting from irradiation (IR), stress, or hypoxia and trigger the activation of purinergic signaling pathways.[4,5] Activation of these receptors serves as a sensor and responder to damage-induced alarm signals and has an important role in modulating tissue homeostasis under stress.[6] Most of the purinergic receptor knockout (KO) mice, including A_{2A}, $P2Y_4$, and $P2Y_2$, display no overt phenotype under homeostatic conditions, but knockdown phenotypes become apparent when KO mice are exposed to stresses or stimuli.[7,8] This indicates that the functional role of purinergic receptors is more apparent under pathophysiological conditions than under homeostatic conditions. Meanwhile, Wells *et al.*[9] showed that purinergic receptors are desensitized upon completion of development, but their expression is upregulated under specific pathophysiological conditions, such as trauma or insults. In line with this, $P2Y_{14}$, a member of the G protein-coupled P2 purinergic receptor family, is expressed at significantly greater levels in fetal hematopoietic stem progenitor cells (HSPCs) as compared with adult HSPCs.[10] In addition, placenta is among the tissues with the highest $P2Y_{14}$ expression compared with most of the other adult tissues.[10] Furthermore, $P2Y_{14}$/ UDP-Glucose (UDP-Glc) axis has also been implicated in various stress responses.[11] These findings suggest a potential role of $P2Y_{14}$ in modulating cellular responses to stress during embryonic development.

Here we demonstrate a novel molecular mediator of the organismal consequences of radiation and show that $P2Y_{14}$ can be manipulated to alter short- and long-term adverse effects of *in utero* IR.

Results

Under homeostatic conditions, heterozygous $(+/-)$ and homozygous $(-/-)$ *P2ry14* mice have normal growth and fertility and exhibit no apparent phenotypic abnormalities. As purinergic receptor signaling is often associated with cellular

[1]Division of Hematology and Oncology, Department of Medicine, University of Pittsburgh Cancer Institute, Hillman Cancer Center, Pittsburgh, PA, USA; [2]Platform Technology and Science (PTS), GlaxoSmithKline, Gunnels Wood Road, Stevenage, SG1 2NY, UK; [3]Department of Radiology, University of Pittsburgh School of Medicine, Pittsburgh, PA, USA; [4]Departmemt of Pathology and Laboratory Medicine, Tulane University School of Medicine, New Orleans, LA 70112, USA; [5]Center for Regenerative Medicine and Cancer Center, Massachusetts General Hospital, Boston, MA, USA; [6]Harvard Stem Cell Institute, Cambridge, MA, USA and [7]Department of Stem Cell and Regenerative Biology, Harvard University, Cambridge, MA, USA
*Corresponding author: B-C Lee, Division of Hematology and Oncology, Department of Medicine, University of Pittsburgh Cancer Institute, Hillman Cancer Center, 5117 Centre Avenue, Pittsburgh, PA 15213, USA. Tel: 412 623 2285; Fax: 412 623 7828; E-mail: leeb4@upmc.edu
[8]These authors contributed equally to this work.
[9]Current address: Institute of Oral Biosciences and School of Dentistry, Chonbuk National University, Jeonju 561-756, Republic of Korea.
Keywords: *in utero* radiation; purinergic receptors; embryo
Abbreviations: UDP-Glc, UDP-Glucose; CT, computed tomography; HSPC, hematopoietic stem progenitor cells; IR, irradiation; TBI, total-body irradiation; p-JNK, phosphorylated JNK; SAPK, stress-activated protein kinases; LSK, lineage negative, Sca-1 positive, c-Kit positive; MRI, magnetic resonance imaging; ROS, reactive oxygen species; KO, knockout
Received 24.1.13; revised 15.4.13; accepted 16.4.13; Edited by A Stephanou

responses to tissue injury,[5] we investigated the potential role of $P2Y_{14}$ to protect cells from genotoxic injury induced by IR. We focus here on the impact of $P2Y_{14}$ on developing embryos, as embryos are highly vulnerable to IR-induced damage and radiation exposure can have profound health consequences later in life. Heterozygous females were mated with heterozygous males. On day 11.5 of pregnancy (E11.5), pregnant females were exposed to total-body irradiation (TBI). Pregnant mice were exposed to various IR regimens. It has been previously shown that doses higher than 1.9 Gy (TBI) lead to embryonic death[12] and we also found that at a dose of 2 Gy TBI none of the $P2Y_{14}$ embryos, regardless of their genotypes, were able to survive to birth. A dose of 1.5 Gy TBI was the maximum dose at which the three mouse genotypes were born at the expected Mendelian ratio without significantly affecting litter size (see Supplementary Results). The litters born to radiation-treated dams did not display any apparent developmental abnormalities and were phenotypically indistinguishable between genotypes during the postnatal period. Litter weights at birth and 3 weeks of age were also not significantly different between genotypes (see Supplementary Results). However, beginning around puberty (between 4 and 6 weeks of age), the majority of *in utero* irradiated wild-type mice began to show retarded growth and weight gain (Figures 1a and b). These mice became moribund and approximately 70–75% of WT offspring died as they reached puberty (Figure 1c). In contrast, a significantly higher percentage of *in utero* irradiated $P2Y_{14}$ homozygous (*P2ry14*$^{-/-}$) mice (60–65%) survived to adulthood with no apparent illness or weight loss through the entire observation period (Figures 1a and c).

Unexpectedly, the treatment of pregnant dams with a putative $P2Y_{14}$ receptor ligand, UDP-Glc, also markedly ameliorated the weight loss and growth retardation observed in *in utero* irradiated WT offspring (Figures 1a and b). UDP-Glc treatment also significantly enhanced postpubertal survival of *in utero* irradiated WT offspring (Figure 1c). This is to some extent surprising, as deficiency of $P2Y_{14}$ receptor endowed offspring with resistance to prenatal radiation. Meanwhile, UDP-Glc did not produce any noticeable effects on growth and survival of $P2Y_{14}$ KO offspring (Figures 1a and c), suggesting that the observed effects of UDP-Glc are likely mediated through a $P2Y_{14}$ receptor-dependent manner.

Hematopoietic tissues, such as thymus, spleen, and bone marrow, are among the most sensitive to radiation. Thus, we examined these tissues in *in utero* irradiated $P2Y_{14}$ offspring. It is known that thymus continues to grow after birth, reaching its maximum size, and weight by the time of puberty but thereafter undergoes involution.[13,14] At the age of 2 weeks, there was no noticeable difference in thymic size between *in utero* irradiated WT and KO offspring (data not shown). Between the ages of 4 and 6 weeks, at which time most prenatally irradiated WT offspring begin to lose their weight, the size of the WT thymus was significantly smaller than those from KO offspring (Figure 2a). The weight and cellularity of the thymus was also found to be drastically reduced in prenatally irradiated WT offspring (Figures 2b and c). The thymic atrophy observed in the WT mice was prevented by the treatment of the pregnant dam with UDP-Glc (Figures 2a and c). Histological examination showed that thymic architecture of *in utero* irradiated WT mice was significantly altered as compared with KO thymus tissue: the WT thymi were disorganized and their cortico-medullary boundary was not as distinct as in KO or UDP-Glc-treated WT thymi (Figure 2d). The magnitude of cell death appeared significantly more

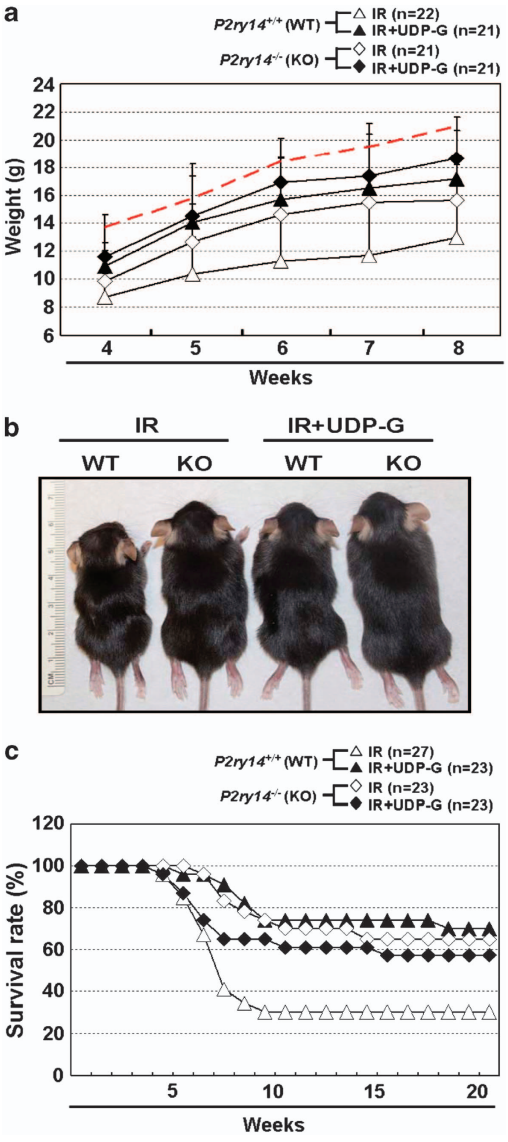

Figure 1 Effects of $P2Y_{14}$ axis on postnatal survival and growth of *in utero* irradiated embryos. (**a**) Body weight of littermates was measured on a weekly basis. With the onset of puberty, the growth rate of WT offspring (white triangles) was significantly retarded compared with KO (white diamonds) as well as UDP-Glc-treated WT offspring (black triangles). In comparison to $P2Y_{14}$ offspring born to dams who were never exposed to prenatal irradiation (see red dashed line), the offspring born to irradiated dams, regardless of genotype, showed a trend toward slightly lower body weights. As body weight can be affected by postmortem dehydration, the results of dead animals were not included in data collection (n = number of animals assessed). We did not measure body weights during neonatal period, as the procedures for genotyping (e.g., tagging and conducting tail biopsy for genomic DNA extraction) before weaning (21 days after birth) increased the risk of cannibalism or abandonment by nursing females. (**b**) Representative images of offspring in each group at 5 weeks of age. (**c**) Survival rate of *in utero* irradiated offspring. WT offspring (white triangles) showed a notably increased incidence of postpubertal mortality as compared with KO (white diamonds) and UDP-Glc-treated WT offspring (black triangles). n = number of animals assessed

pronounced in the thymocytes derived from *in utero* irradiated WT offspring, as compared with counterpart cells from their KO offspring (Figure 2e). UDP-Glc was also effective in rescuing the WT thymocytes from cell death (Figure 2e). When the thymocytes were analyzed for CD4 and CD8 expression, WT offspring displayed a reduction in the relative percentage of $CD4^+CD8^+$ cells as compared with KO or UDP-Glc-treated WT counterparts (Figure 2f, left panel). In the thymi of WT offspring, the absolute numbers of all subsets were significantly decreased (Figure 2f, right panel). Thymocytes from prenatally irradiated WT offspring consistently exhibited increased levels of cell death in all subsets of thymocytes rather than showing a preferential cell death in a specific subset (Figure 2g). Interestingly, when WT thymocytes were exposed *in vitro* to various doses of IR, there was dose-dependent increase of cell surface expression of P2Y$_{14}$ receptor, suggesting a potential causal relationship between P2Y$_{14}$ receptor expression and radiation response (Figure 2h).

Radiation raises reactive oxygen species (ROS) levels in cells, leading to cellular damage. As expected, IR led to significant increase in the levels of mitochondrial superoxide in WT thymocytes (Figure 2i). In contrast, low levels of mitochondrial superoxide were detected in the KO. Treatment with UDP-Glc resulted in a significant decrease in mitochondrial superoxide in irradiated WT thymocytes. ROS often triggers stress-activated protein kinases (SAPK)-promoting apoptotic cell death. We found that thymocytes from prenatally irradiated WT offspring have higher levels of phosphorylated JNK (p-JNK) and p38 MAPK, compared with their KO counterparts (Figure 2j). The levels of phosphorylated ERK in WT thymocytes were slightly but not significantly lower than that of the KO thymocytes. Administration of

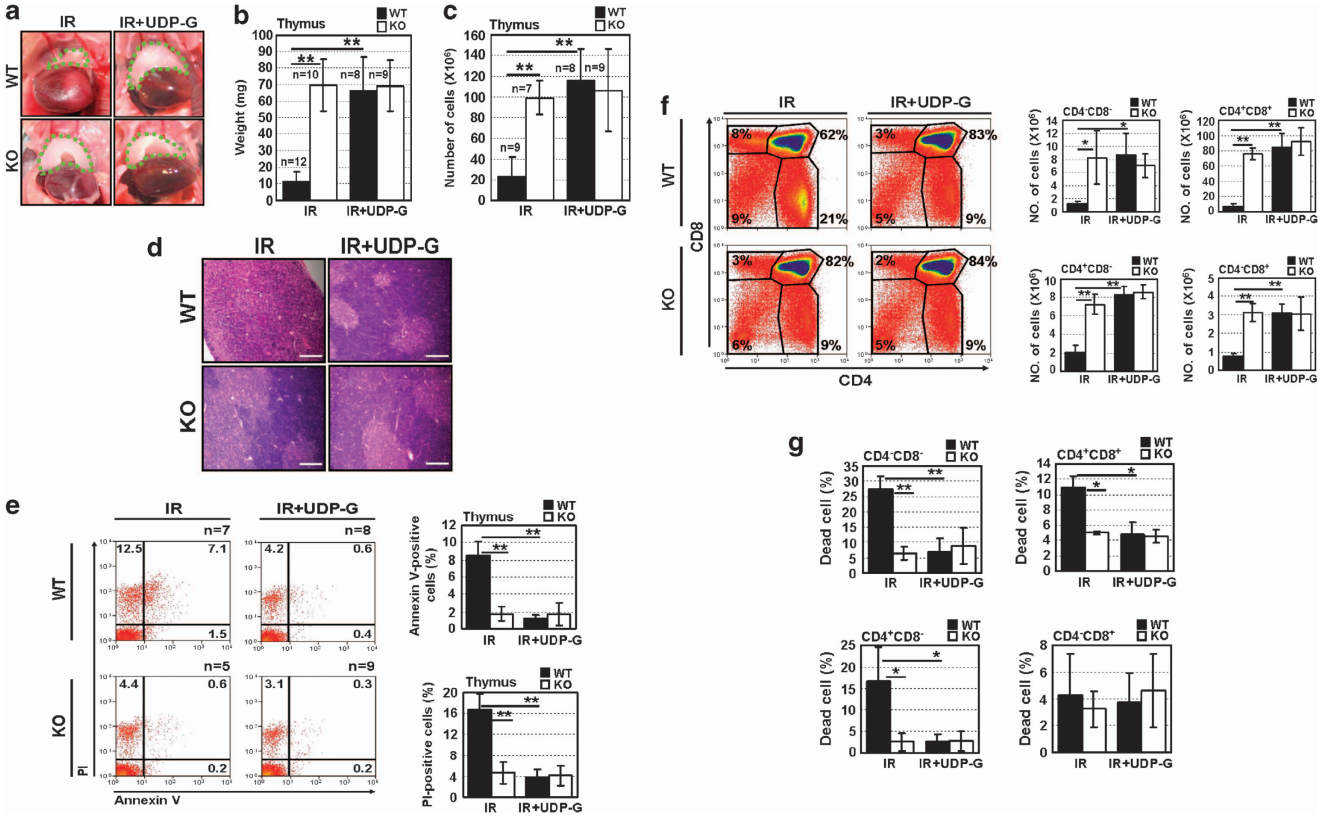

Figure 2 Effects of P2Y$_{14}$ axis on thymic atrophy induced by prenatal irradiation. (**a**) Macroscopic appearance of thymus at 5 weeks of age: thymic tissue is outlined with dotted lines. Thymus was harvested from 4- to 6-week-old mice, and weight (**b**) and total thymic numbers (**c**) were determined. $n=$number of animals tested. $^{**}P<0.01$. (**d**) Comparison of histological analysis of thymus; thymic tissues isolated from each group were stained with hematoxylin-eosin. Note that thymi from WT offspring exhibit severe structural anomalies. Shown is representative staining of thymic sections from offspring born to prenatally irradiated dams. Scale bar: 200 μm; (**e**) Thymic cells were stained with Annexin V and PI. Percentages of gated cell populations are indicated. The accompanying graphs show the percentage of Annexin V + and PI + thymic cells. $n=$number of animals tested. $^{**}P<0.01$. (**f**) CD4/CD8 profile of thymocytes of indicated mice at 4–6 weeks of age. Thymocytes were stained with antibodies to CD4 and CD8. The graphs show the absolute number of cells in indicated subsets. For each group, more than three mice were individually analyzed. $^{*}P<0.05$, $^{**}P<0.01$. (**g**) Cell death of thymocyte subsets was analyzed by flow cytometry as described above. The graphs show the percentage of PI-positive cells of indicated subsets. For each group, more than three mice were individually analyzed. $^{*}P<0.05$, $^{**}P<0.01$. (**h**) Thymocytes were prepared from 4- to 6-week-old wild-type mice and exposed *in vitro* to different doses of γ-irradiation as indicated. Cells were stained with biotinylated anti-P2Y14 antibody and APC-conjugated streptavidin. Percentages of gated cell populations are indicated. The accompanying graphs show the percentage of P2Y14 + thymic cells. (**i**) Levels of mitochondrial superoxide in thymic cells were measured by using Mitosox Red. Percentages of gated cell populations are indicated. The accompanying graphs show the percentage of Mitosox Red-stained thymic cells. (**j**) Western blot analysis in thymic cells. Thymic cell extracts isolated from indicated mice at 4–6 weeks of age were analyzed by western blot analysis using the antibodies as indicated. The numerical values in the accompanying table represent fold difference in p53 and p21 expression relative to prenatally irradiated WT offspring after normalization to β-actin-loading control, as determined by densitometry. (**k**) Immunohistochemical staining of prenatally irradiated thymic tissues with anti-p53 (left panel) and anti-p21 (right panel). Red arrows indicate representative positively stained cells. Scale bar: 20 μm

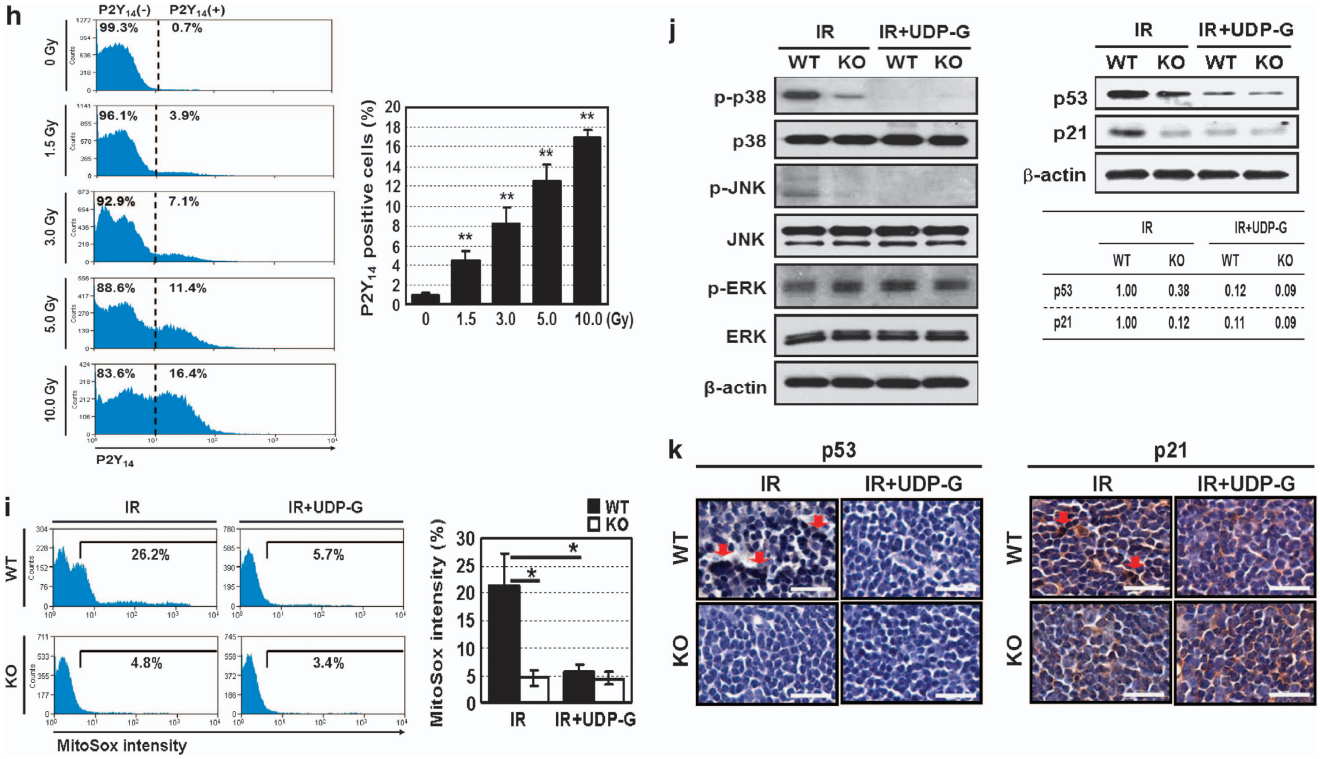

Figure 2 Continued

UDP-Glc markedly reduced the levels of p-JNK and p38 MAPK activation in the WT thymocytes. p53 is a critical downstream target of JNK and p38 MAPK and is required for radiation-induced apoptosis in mouse thymocytes.[15] As shown in Figure 2j (see right panels), *in utero* irradiated WT thymocytes expressed higher levels of p53 protein compared with that of *in utero* irradiated KO thymocytes. The immediate downstream p53 target, p21, was also upregulated in the thymocytes of prenatally irradiated WT offspring. However, when $P2Y_{14}$ dams were treated with UDP-Glc, a significant decrease in expression of p53 and p21 was noted in WT thymocytes. The observed changes in p53 and p21 expression were further confirmed by immunohistochemical analysis (Figure 2k).

A similar difference was observed for spleen: at 5–6 weeks of age, the spleens of *in utero* irradiated WT mice were significantly decreased in size and weight as compared with those of KO or UDP-Glc-treated WT mice (Figures 3a and b). The absolute number of cells per spleen was also significantly reduced in prenatally irradiated WT offspring (Figure 3c) and this coincided with the increased percentage of apoptotic and dead cells in the WT splenocytes (Figure 3d). UDP-Glc treatment was able to rescue a significant portion of splenocytes from undergoing the cell death pathway in the WT offspring (Figure 3d). As similarly observed in thymocytes, the levels of p53 and p21 were greater in the wild-type spleen cells as compared with their KO littermate counterparts. Similarly, UDP-Glc was able to abrogate p53 and p21 induction in the WT spleen cells (Figure 3e).

Nucleated bone marrow cell counts were also reduced in the WT offspring of $P2Y_{14}$ dams exposed *in utero* to IR (Figure 4a). As HSPCs, the source of the blood cells in the bone marrow, are primarily responsible to maintain bone marrow homeostasis, we further analyzed a subset of HSPCs (Lin −, Sca-1 +, c-Kit +, hereafter referred to as LSK cells). Similarly, the WT offspring showed a statistically significant decrease in their absolute number of LSK cells as compared with the counterpart cells from KO offspring (Figure 4b). This was accompanied by a modest but statistically significant increase in cell death in the WT LSK cells (Figure 4c, right panel). Thus, the reduction in bone marrow cellularity observed in the WT offspring appears to be related to the reduction of their HSPC populations by cell death. Notably, the majority of dead cells observed in WT LSK cells were Annexin V − and PI + cells (Figure 4c), suggesting the possibility that WT LSK cells die via a non-apoptotic pathway. UDP-Glc was effective in reducing cell death in the WT LSK cells (Figure 4c, right panel) and resulted in a significant recovery in the absolute number of WT LSK cells (Figure 4b). Western blot analysis of p53 or p21 levels in LSK cells was not technically feasible due to their low frequency. Intriguingly, whereas HSPCs from *in utero* irradiated $P2Y_{14}$ KO offspring were more resistant to prenatal IR-induced cell death, they tend to undergo cellular senescence (Figure 4d). As many cell types acquire resistance to certain cell death stimuli upon entering the state of senescence,[16] it is a conceivable possibility that a subtype of $P2Y_{14}$ KO HSPCs may engage senescence as an attempt to escape IR-induced cell death. Bone marrow cells from *in utero* irradiated $P2Y_{14}$ WT mice, despite of their high susceptibility to prenatal IR-induced cell death, were able to compete almost equally with competitor cells up to 1 year post-transplant (46% *versus* 54%; Figure 4e,

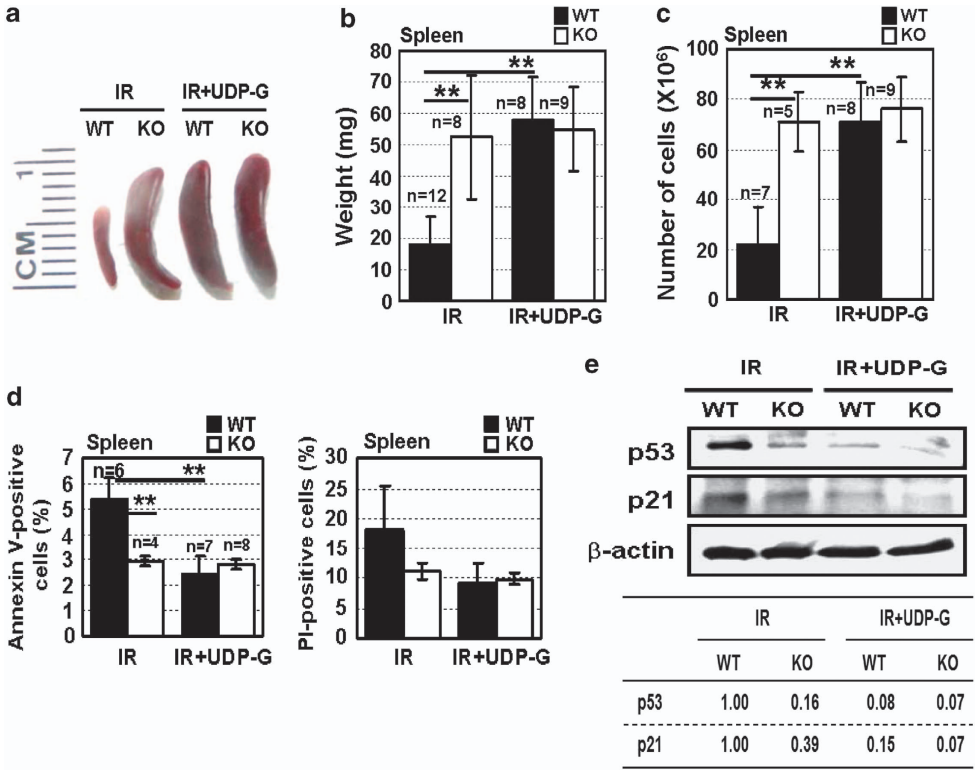

	IR		IR+UDP-G	
	WT	KO	WT	KO
p53	1.00	0.16	0.08	0.07
p21	1.00	0.39	0.15	0.07

Figure 3 Effects of $P2Y_{14}$ axis on splenic atrophy induced by prenatal irradiation. Spleens were isolated from prenatally irradiated offspring at 4–6 weeks of age. (**a**) Macroscopic appearance of spleen at 5 weeks of age. Spleen weights (**b**) and total number of spleen cells (**c**) were determined. n = number of animals tested. $^{**}P<0.01$. (**d**) Cell death of splenic cells was examined by flow cytometry analysis as described above. n = number of animals tested. $^{**}P<0.01$. (**e**) Western blot analysis of p53 and p21 protein levels in spleen cells. The protein levels were determined as described in the legend of Figure 2j

upper panel). In contrast, bone marrow cells from *in utero* irradiated $P2Y_{14}$ KO mice competed poorly with competitor cells (Figure 4e, lower panel; 24% *versus* 76%). This is probably due, in part, to a greater proportion of senescent HSPCs in KO bone marrow as shown in Figure 4d.

It was previously shown that prenatal exposure to radiation can damage the developing brain of unborn babies and cause hydrocephalus and/or mental retardation.[17] The prenatally irradiated WT offspring were easily distinguishable from their KO littermates, as WT offspring exhibited a higher incidence of hydrocephalus with an enlarged domed cranium (Figure 5a). The percentage of the WT offspring showing clear signs of hydrocephalus was approximately 70%, which is more than twofold higher incidence than that of the KO offspring (70% *versus* 31%). UDP-Glc treatment reduced the incidence and severity of hydrocephalus by nearly 30–35% in prenatally irradiated WT offspring (Figures 5a and b). For further analysis, magnetic resonance imaging (MRI) was performed with prenatally irradiated WT and KO offspring. MRI image demonstrates significant hydrocephalus and/or edema, resulting in internal hydrocephalus in *in utero* irradiated WT mice (Figure 5c). In contrast, MRI of *in utero* irradiated KO mice exhibited very little or no hydrocephalus (Figure 5c). The treatment of pregnant dam with UDP-Glc was able to significantly reduce the severity of IR-induced hydrocephalus in the WT offspring (Figure 5c). Of note, the morphological signs of hydrocephalus such as a rounded and enlarged cranium were apparent by 1–2 weeks of age. A similar trend was observed for p53 and p21 protein expression in the prenatally irradiated brain tissues (Figure 5d).

Discussion

$P2Y_{14}$-null embryos exhibit a marked resistance to tissue injury induced by *in utero* IR. Considering that the presence of $P2Y_{14}$ receptor makes embryos more susceptible to the *in utero* radiation, it was anticipated that the activation of $P2Y_{14}$ axis by exogenous UDP-Glc would lead to even more tissue damage increasing pre- and post-natal mortality of prenatally irradiated WT embryos. However, unexpectedly, UDP-Glc significantly ameliorated IR-induced tissue injury in prenatally irradiated WT mice and led to an increased postpubertal survival rate. A ligand can behave either as agonist or antagonist for the same protein depending upon both ligand concentration and cell context. In this context, UDP-Glc appears to phenocopy gene deletion and therefore has an inhibitory effect. There are a number of explanations for this including serving as a true antagonist, desensitization of the receptor or competition with cognate ligand.

It is not clear why most phenotypic differences between WT and KO offspring do not appear until puberty. The molecular events governing fate decisions in *in utero* irradiated embryo or fetus are difficult to dissect due to its complexity, including reciprocal interactions between the mother and the embryo. Nevertheless, given that the effects of prenatal radiation often

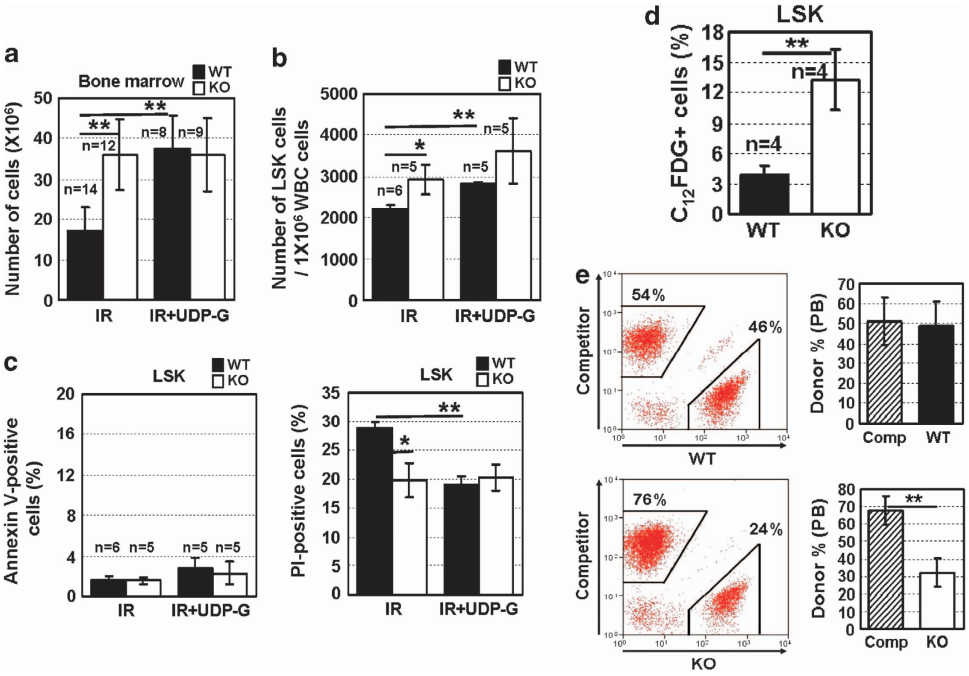

Figure 4 Effects of P2Y$_{14}$ axis on bone marrow cellularity induced by prenatal irradiation. Bone marrow cells were isolated from prenatally irradiated offspring at 5 weeks of age. (**a**) Total number of nucleated cells in the bone marrow isolated from indicated mice. $n=$ number of animals tested. (**b** and **c**) Bone marrow cells were stained with a lineage marker cocktail, c-Kit, Sca-1 (LSK), Annexin-V and PI. Absolute number of LSK cells in the bone marrow of indicated offspring is shown in **b**. (**c**) Cell death analysis on the gated LSK cells: the graphs show the mean percentage of Annexin-V (left panel) and PI (right panel)-positive cells of indicated subsets. $n=$ number of animals tested. (**d**) LSK cells isolated from prenatally irradiated WT and KO offspring at 5 weeks of age were gated for the comparison of senescence associated-β-Gal activity. $^{**}P<0.01$. (**e**) For competitive repopulation assays, bone marrow cells (2×10^6) from *in utero* irradiated wild-type and KO (B6, CD45.2) mice were mixed with equal number of competitor bone marrow cells derived from congenic mice (B6, CD45.1) and transplanted into lethally irradiated recipients (CD45. 1/2). Peripheral blood was analyzed for donor contribution using CD45 markers. The histograms (left panels) and graphs (right panels) show the relative contributions of test (CD45.2) *versus* competitor (CD45.1) populations in peripheral blood of mice at 1 year post-transplant. $^{**}P<0.01$

emerge later in life, our study more closely recapitulates what is encountered in clinical setting.

The ability of P2Y$_{14}$ to mediate sensitivity of fetal mice and multiple tissues therein to radiation injury is a striking finding. Although modulating other molecules such as p53 and PUMA has been shown to alter cell sensitivity to radiation damage,[15,18–20] a cell surface receptor doing so is particularly distinctive and, we would argue, of significant importance as it represents a potentially targetable means of affecting the consequences of radiation injury. The demonstration that UDP-Glc can mimic P2Y$_{14}$ deletion is of special interest in that regard. The UDP-Glc data demonstrate the feasibility of using a simple pharmacologic intervention to modulate significant consequences at a cellular, tissue and organismal level. It is therefore possible to envision the use of an agent like UDP-Glc or other P2Y$_{14}$ inhibitors in the context of radiation exposure in pregnancy.

Materials and Methods

Animals. *P2ry14* KO mice[21] were kindly provided under MTA by GlaxoSmithKline (Brentford, Middlesex, UK). The mice were backcrossed to C57BL/6 for at least nine generations (N9). Heterozygote male and female mice were mated, and pregnant dams were exposed to a 1.5-Gy dose of whole-body irradiation (TBI) at day 11.5 of gestation. Dose from conventional CT scan is generally less than 2–3 cGy. Pregnant dams exposed to this dose of TBI did not show any sign of weight loss or illness, and there were no notable changes in their fertility over time. The genotyping was performed by PCR analysis with provided primer sets: wild-type: 5′-AGCCCCTTC TGACGTCTATTGTGC-3′, 5′-ATTGCGGCTGGACTTCCTCTTGAC-3′; 30 cycles of 94 °C for 45 s, 55 °C for 45 s, and 72 °C for 60 s (329 bp) or 5′-ACTGGGCAAA ACACCTTCAC-3′, 5′-GTGTAGGGGATTCTGGCAAT-3′; 30 cycles of 94 °C for 30 s, 54 °C for 60 s, and 72 °C for 30 s (240 bp) mutant 5′-CCGGCCGCTTGGGTG GAGAGG-3′, 5′-TCGGCAGGAGCAAGGTGAGATGACA-3′; 30 cycles of 94 °C for 30 s, 68 °C for 30 s, 72 °C for 30 s (299 bp) or 5′-CTACCCGTGATATTGCTGAAG AGCTTGGCG-3′, 5′ AAATAGATACGAGTGTTGCTTGGAA-3′; 30 cycles of 94 °C for 30 s, 62 °C for 30 s, 72 °C for 30 s (600 bp). Unless otherwise stated, all experiments were performed with littermates as control. All analysis unless otherwise specified in the text were performed on the offspring that were killed at the age of 4–6 weeks. Spleen and thymus were harvested from 4- to 6-week-old mice. All studies were conducted after review by the GSK and University of Pittsburgh's Institutional Animal Care and Use Committee and in accordance with the GSK and University of Pittsburgh's Policy on the Care, Welfare, and Treatment of Laboratory Animals.

UDP-glucose treatment. UDP-glucose was dissolved in endotoxin-free PBS just before giving the injection. IR exerts its cytotoxicity in large part through the generation of ROS. Although ROS levels increased immediately following IR, persistent oxidative stress has also been reported.[22] Pregnant dams were given subcutaneous injections of UDP-Glc (200 mg/kg body weight, Sigma-Aldrich, St Louis, MO, USA) 1 h before and immediately after TBI (1.5 Gy; to reduce a potential oxidative damage during the early post-IR period), and then once daily for 2 days (to mitigate persistent oxidative stress). The rationale for this injection schedule is also based on the result of previous studies in which radiation-protective agents are administered both before and after radiation exposure.[23,24]

Flow cytometry analysis. Single-cell suspensions were made from the thymus, spleen, and bone marrow of 4- to 6-week-old mice and analyzed by flow cytometry as previously described.[25] For HSPC analysis, bone marrow cells were stained with a lineage marker cocktail, c-Kit, and Sca-1 (e-Bioscience, San Diego, CA, USA). Thymocytes were stained with antibodies to P2Y$_{14}$ (Alomone Labs,

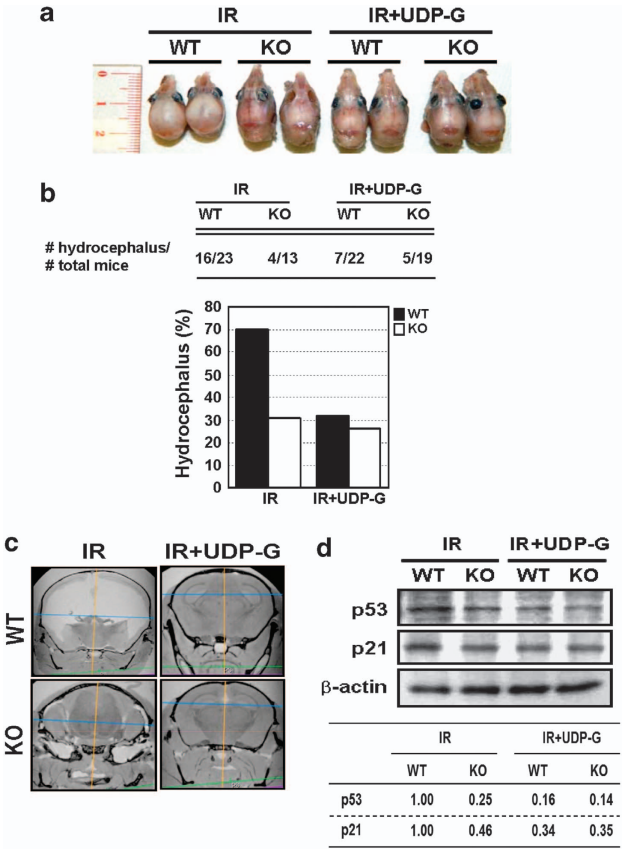

Figure 5 Effects of $P2Y_{14}$ axis on incidence of hydrocephalus induced by prenatal irradiation. (**a**) WT offspring develop severe hydrocephalus displaying rounded and domed cranium. KO offspring show grossly normal cranium. Note that exogenous UDP-Glc significantly reduced the severity of hydrocephalus. (**b**) The following table and graph show the number and percentage of offspring with obvious physical signs of hydrocephalus. (**c**) Coronal view of brain MRI image of prenatally irradiated offspring. MRI of the WT offspring clearly revealed a large cystic lesion. (**d**) Western blot analysis of p53 and p21 protein levels in brain cells. The protein levels were determined as described in the legend of Figure 2j

Jerusalem, Israel), CD4 and CD8 (e-Bioscience). Cell death was assessed using Annexin-V-PI double staining, according to the manufacturer's instructions (BD Pharmingen, San Jose, CA, USA). Levels of mitochondrial superoxide in thymic cells were measured by using Mitosox Red (Invitrogen, Grand Island, NY, USA). Cellular senescence was assessed by measuring senescence associated (SA)-β-gal activity (use 5-dodecanoylaminofluorescein di-b-D-galactopyranoside as a fluorogenic substrate) in the lineage$-$, Sca-1$+$, c-Kit$+$ (LSK)-gated bone marrow cells as previously described.[26]

Western blot analysis. Equal amounts of total protein (20 μg) for each sample were analyzed by western blotting. The blots were probed with primary antibodies overnight at 4 °C followed by horseradish peroxidase-conjugated secondary antibodies. The blots were developed, exposed, and analyzed using Un-scan-IT image analysis software (Orem, UT, USA). Phospho-p38 MAPK (cat. #9211), p38 MAPK (cat. #9212), phospho-SAPK/JNK (cat.#9251), SAPK/JNK (cat. #9258), phospho-ERK (cat. #9101), and ERK (cat. #9102) were purchased from Cell Signaling (Danvers, MA, USA) and p53 (sc-6243) and p21 (sc-6246) were purchased from Santa Cruz Biotechnology (Dallas, TX, USA).

Competitive repopulation assays. For competitive repopulation assays, bone marrow cells (2×10^6) from *in utero* irradiated wild-type and KO (B6, CD45.2) mice were mixed with equal number of competitor bone marrow cells derived from congenic mice (B6, CD45.1) and transplanted into lethally irradiated recipients (CD45. 1/2, 6–8 weeks old). Peripheral blood was analyzed for donor contribution using CD45 markers.

MRI. The mice were killed and fixed by transcardiac perfusion with paraformaldehyde and 5% ProHance (Bracco Diagnostics, Inc., Monroe Township, NJ, USA) following the technique described by Johnson, *et al.*[27] After perfusion, the heads were separated from the body, skinned, and placed in a solution of paraformaldehyde/ProHance. MRI images were obtained on a 7-T Clinscan animal MRI system with a 3D FLASH sequence TE 2.7 ms, TR 26 ms, tip angle 35°, 8 averages, and 0.08 mm isotropic resolution (FOV: 15.62 $\times$ 20.00 $\times$ 16.64, *W,H,D*; 200 $\times$ 256 $\times$ 208).

Conflict of Interest

The authors declare no conflict of interest.

Acknowledgements. We thank Drs. Seong-Gi Kim and Saiful Huq for the helpful discussions and suggestions. This study was supported in part by research funding from the Department of Defense (W81XWH-09-1-0364) to B-C Lee. This project used the UPCI flow cytometry and animal facility, which were supported in part by the P30CA047904 award from NIH.

1. Lazarus E, Debenedectis C, North D, Spencer PK, Mayo-Smith WW. Utilization of imaging in pregnant patients: 10-year review of 5270 examinations in 3285 patients–1997-2006. *Radiology* 2009; **251**: 517–524.
2. Burnstock G. Discovery of purinergic signalling, the initial resistance and current explosion of interest. *Br J Pharmacol* 2012; **167**: 238–255.
3. Glaser T, Resende RR, Ulrich H. Implications of purinergic receptor-mediated intracellular calcium transients in neural differentiation. *Cell Commun Signal* 2013; **11**: 12.
4. Abbracchio MP, Burnstock G. Purinergic signalling: pathophysiological roles. *Jpn J Pharmacol* 1998; **78**: 113–145.
5. Tsukimoto M, Homma T, Ohshima Y, Kojima S. Involvement of purinergic signaling in cellular response to gamma radiation. *Radiat Res* 2010; **173**: 298–309.
6. Rossi L, Salvestrini V, Ferrari D, Di Virgilio F, Lemoli RM. The sixth sense: hematopoietic stem cells detect danger through purinergic signaling. *Blood* 2012; **120**: 2365–2375.
7. Chen JF, Huang Z, Ma J, Zhu J, Moratalla R, Standaert D *et al.* A(2 A) adenosine receptor deficiency attenuates brain injury induced by transient focal ischemia in mice. *J Neurosci* 1999; **19**: 9192–9200.
8. Matos JE, Robaye B, Boeynaems JM, Beauwens R, Leipziger J. K$+$ secretion activated by luminal P2Y2 and P2Y4 receptors in mouse colon. *J Physiol* 2005; **564**(Pt 1): 269–279.
9. Wells DG, Zawisa MJ, Hume RI. Changes in responsiveness to extracellular ATP in chick skeletal muscle during development and upon denervation. *Dev Biol* 1995; **172**: 585–590.
10. Lee BC, Cheng T, Adams GB, Attar EC, Miura N, Lee SB *et al.* P2Y-like receptor, GPR105 (P2Y14), identifies and mediates chemotaxis of bone-marrow hematopoietic stem cells. *Genes Dev* 2003; **17**: 1592–1604.
11. Lazarowski ER, Shea DA, Boucher RC, Harden TK. Release of cellular UDP-glucose as a potential extracellular signaling molecule. *Mol Pharmacol* 2003; **63**: 1190–1197.
12. Dekaban AS. Effects of x-radiation on mouse fetus during gesttion: emphasis on distribution of cerebral lesions, Part II. *J Nucl Med* 1969; **10**: 68–77.
13. Heikenwalder M, Prinz M, Zeller N, Lang KS, Junt T, Rossi S *et al.* Overexpression of lymphotoxin in T cells induces fulminant thymic involution. *Am J Pathol* 2008; **172**: 1555–1570.
14. Martiney MJ, Rulli K, Beaty R, Levy LS, Lenz J. Selection of reversions and suppressors of a mutation in the CBF binding site of a lymphomagenic retrovirus. *J Virol* 1999; **73**: 7599–7606.
15. Lowe SW, Schmitt EM, Smith SW, Osborne BA, Jacks T. p53 is required for radiation-induced apoptosis in mouse thymocytes. *Nature* 1993; **362**: 847–849.
16. Campisi J, d'Adda di Fagagna F. Cellular senescence: when bad things happen to good cells. *Nat Rev Mol Cell Biol* 2007; **8**: 729–740.
17. Gilbert-Barness E. Teratogenic causes of malformations. *Ann Clin Lab Sci* 2010 Spring **40**: 99–114.
18. Kastan MB, Onyekwere O, Sidransky D, Vogelstein B, Craig RW. Participation of p53 protein in the cellular response to DNA damage. *Cancer Res* 1991; **51**(23 Pt 1): 6304–6311.
19. Yu H, Shen H, Yuan Y, XuFeng R, Hu X, Garrison SP *et al.* Deletion of Puma protects hematopoietic stem cells and confers long-term survival in response to high-dose gamma-irradiation. *Blood* 2010; **115**: 3472–3480.
20. Qiu W, Carson-Walter EB, Liu H, Epperly M, Greenberger JS, Zambetti GP *et al.* PUMA regulates intestinal progenitor cell radiosensitivity and gastrointestinal syndrome. *Cell Stem Cell* 2008; **2**: 576–583.
21. Bassil AK, Bourdu S, Townson KA, Wheeldon A, Jarvie EM, Zebda N *et al.* UDP-glucose modulates gastric function through P2Y14 receptor-dependent and -independent mechanisms. *Am J Physiol Gastrointest Liver Physiol* 2009; **296**: G923–G930.
22. Zhao W, Diz DI, Robbins ME. Oxidative damage pathways in relation to normal tissue injury. *Br J Radiol* 2007; **1**: S23–S31.

23. Jia D, Koonce NA, Griffin RJ, Jackson C, Corry PM. Prevention and mitigation of acute death of mice after abdominal irradiation by the antioxidant N-acetyl-cysteine (NAC). *Radiat Res* 2010; **173**: 579–589.
24. Liu Y, Zhang H, Zhang L, Zhou Q, Wang X, Long J *et al.* Antioxidant N-acetylcysteine attenuates the acute liver injury caused by X-ray in mice. *Eur J Pharmacol* 2007; **575**: 142–148.
25. Metcalf D, Di Rago L, Mifsud S, Hartley L, Alexander WS. The development of fatal myocarditis and polymyositis in mice heterozygous for IFN-gamma and lacking the SOCS-1 gene. *Proc Natl Acad Sci USA* 2000; **97**: 9174–9179.
26. Cho J, Shen H, Yu H, Li H, Cheng T, Lee SB *et al.* Ewing sarcoma gene Ews regulates hematopoietic stem cell senescence. *Blood* 2011; **117**: 1156–1166.
27. Johnson GA, Ali-Sharief A, Badea A, Brandenburg J, Cofer G, Fubara B *et al.* High-throughput morphologic phenotyping of the mouse brain with magnetic resonance histology. *Neuroimage* 2007; **37**: 82–89.

Supplementary Information accompanies this paper on Cell Death and Disease website (http://www.nature.com/cddis)